π, K^+, and K^0 electromagnetic form factors

Pieter Maris and Peter C. Tandy
Center for Nuclear Research, Department of Physics, Kent State University, Kent, Ohio 44242
(Received 5 May 2000; published 20 October 2000)

The rainbow truncation of the quark Dyson-Schwinger equation is combined with the ladder Bethe-Salpeter equation for the meson amplitudes and the dressed quark-photon vertex in a self-consistent Poincaré-invariant study of the pion and kaon electromagnetic form factors in impulse approximation. We demonstrate explicitly that the current is conserved in this approach and that the obtained results are independent of the momentum partitioning in the Bethe-Salpeter amplitudes. With model gluon parameters previously fixed by the chiral condensate, the pion mass and decay constant, and the kaon mass, the charge radii and spacelike form factors are found to be in good agreement with the experimental data.

PACS number(s): 24.85.+p, 14.40.Aq, 13.40.Gp, 11.10.St

I. INTRODUCTION

The light pseudoscalar mesons play an important role in understanding low-energy QCD. They are the lightest observable hadronic bound states of a quark and an antiquark, and are the Goldstone bosons associated with chiral symmetry breaking. Their static properties such as the mass and decay constants have been studied extensively and are qualitatively understood within QCD. A number of studies of pseudoscalar mesons [1,2] have played a key role in the development of continuum methods for modeling QCD via the Dyson-Schwinger equations (DSEs). Such methods have now evolved into an excellent tool for the study of nonperturbative aspects of a variety hadronic properties and processes in QCD [3]. Dynamic properties and scattering observables continue to pose a difficult challenge. In this respect, the elastic electromagnetic form factors of the pion and kaon are very interesting: the probe is well understood, there are accurate data for F_π at low Q^2, and the charge radii r_π^2, $r_{K^+}^2$, and $r_{K^0}^2$ are experimentally known. Currently, there are several experiments at JLab to determine both the pion and the kaon form factor in the range $0.5 < Q^2 < 3\ \mathrm{GeV}^2$ to higher accuracy [4,5], and this may provide better discrimination between different theoretical models.

In this work, we use the DSEs to calculate the pion and kaon electromagnetic form factors in impulse approximation. We obtain the meson Bethe-Salpeter amplitudes (BSAs) and the quark-photon vertex as solutions of the homogeneous and inhomogeneous Bethe-Salpeter equations (BSEs) in ladder truncation. The required dressed quark propagators are obtained from solutions of the quark DSE in rainbow truncation. Nonanalytic effects from vector mesons are automatically taken into account, because these vector $q\overline{q}$ bound states appear as poles in the quark-photon vertex solution [6]. We employ a realistic model for the effective quark-antiquark coupling that has been shown to reproduce the pion and kaon masses and decay constants [2] as well as the masses and decay constants for the vector mesons ρ, ϕ, and $K^\star$ to within 10% [7]. The model parameters are fixed in previous work [7] and constrained only by m_π, m_K, f_π, and $\langle \overline{q}q \rangle$. The produced pion charge radius is within 2% of the experimental value [6]. Here, we use the same approach, without parameter adjustment, to calculate the neutral and charged kaon form factors and charge radii; we also extend our previous pion form factor calculations [6] to the spacelike Q^2 domain anticipated for future JLab [5] data.

This approach is consistent with quark and gluon confinement [3,8], generates dynamical chiral symmetry breaking [9], and is Poincaré invariant. It is straightforward to implement the correct one-loop renormalization group behavior of QCD [2], and to obtain agreement with perturbation theory in the perturbative region. Provided that the relevant Ward identities are preserved in the truncation of the DSEs, the corresponding currents are conserved. Axial current conservation ensures the Goldstone nature of the pions and kaons [10]; electromagnetic current conservation ensures the correct hadronic charge without fine-tuning.

In Sec. II we review the formulation that underlies a description of the pion and kaon charge form factors within a modeling of QCD through the DSEs. Within the impulse approximation, we outline the manner in which ladder-rainbow dynamics for the propagators, BSAs and quark-photon vertex produces a conserved meson electromagnetic current. We also indicate the corrections to the impulse approximation that are needed to maintain current conservation when the truncation of the DSEs goes beyond rainbow-ladder level. In Sec. III we discuss the details of the model and present our numerical results for the form factors. Concluding remarks are given in Sec. IV.

II. PSEUDOSCALAR ELECTROMAGNETIC FORM FACTORS

The three-point function describing the coupling of a photon with momentum Q to a pseudoscalar meson, with initial and final momenta $P_\pm = P \pm Q/2$, can be written as the sum of two terms

$$\Lambda_\nu^{a\overline{b}}(P,Q) = \hat{Q}^a \Lambda_\nu^{a\overline{b}a}(P,Q) + \hat{Q}^{\overline{b}} \Lambda_\nu^{a\overline{b}\overline{b}}(P,Q), \qquad (1)$$

where $\hat{Q}$ is the quark or antiquark electric charge, and where $\Lambda^{a\overline{b}a}$ and $\Lambda^{a\overline{b}\overline{b}}$ describe the coupling of a photon to the quark (a) and antiquark ($\overline{b}$), respectively. The meson form factor is defined by

$$\Lambda_\nu^{a\bar{b}}(P,Q) = 2\,P_\nu\; F(Q^2), \tag{2}$$

and the corresponding charge radius is $r^2 = -6F'(Q^2)$ with $Q^2=0$. Analogously, we can define a form factor for each of the two terms on the right-hand side of Eq. (1), for example

$$\Lambda_\nu^{a\bar{b}b}(P,Q) = 2\,P_\nu\; F_{a\bar{b}}(Q^2). \tag{3}$$

Current conservation dictates that each of the form factors $F_{a\bar{b}}(Q^2)$ and $F_{a\bar{a}}(Q^2)$ is 1 at $Q^2=0$.

A. Impulse approximation

The impulse approximation allows form factors to be described in terms of dressed quark propagators, bound state BSAs, and the dressed $qq\gamma$ vertex. We denote by $\Gamma_\mu^a(q,q';Q)$ the quark-photon vertex describing the coupling of a photon with momentum Q to a quark of flavor a with final and initial momenta q and $q'=q-Q$, respectively. With this notation, the vertices in Eq. (1) take the form[1]

$$\begin{aligned}\Lambda_\nu^{a\bar{b}b}(P,Q) = N_c \int^\Lambda \frac{d^4k}{(2\pi)^4} \mathrm{Tr}[& S^a(q)\,\Gamma^{a\bar{b}}(q,q_+;P_-) \\ & \times S^b(q_+)\, i\Gamma_\nu^b(q_+,q_-;Q) \\ & \times S^b(q_-)\,\bar{\Gamma}^{a\bar{b}}(q_-,q;-P_+)],\end{aligned} \tag{4}$$

where $q=k+\frac{1}{2}P$, $q_\pm = k-\frac{1}{2}P\pm\frac{1}{2}Q$, and $P_\pm = P\pm\frac{1}{2}Q$. The expression for Λ_ν^{aba} is analogous. The notation $\int^\Lambda$ denotes a translationally-invariant regularization of the integral, where Λ is the regularization mass scale. The regularization can be removed at the end of all calculations, after renormalization, by taking the limit $\Lambda\to\infty$. $S(q)$ is the dressed quark propagator, $\Gamma^{a\bar{b}}(q,q';P)$ is the meson BSA with on-shell momentum $P^2=-m^2$ and quark and antiquark momenta q and $q'=q-P$, respectively.

Both $S(q)$ and $\Gamma^{a\bar{b}}(q,q';P)$ are solutions of their respective DSEs

$$\begin{aligned}S(p)^{-1} = Z_2\, i\not{p} + Z_4\, m(\mu) + Z_1 \int^\Lambda \frac{d^4q}{(2\pi)^4} g^2 D_{\mu\nu} \\ \times (p-q)\frac{\lambda^i}{2}\gamma_\mu S(q)\Gamma_\nu^i(q,p)\end{aligned} \tag{5}$$

and

$$\Gamma^{a\bar{b}}(p,p';Q) = \int^\Lambda \frac{d^4q}{(2\pi)^4} K(p,q;Q)\,\chi^{a\bar{b}}(q,q';Q), \tag{6}$$

where $D_{\mu\nu}(k)$ is the renormalized dressed-gluon propagator, $\Gamma_\nu^i(q,p)$ is the renormalized dressed quark-gluon vertex, K is the renormalized $\bar{q}q$ scattering kernel that is irreducible with respect to a pair of $\bar{q}q$ lines, and $\chi^{a\bar{b}}(q,q';Q) = S^a(q)\Gamma^{a\bar{b}}(q,q';Q)S^b(q')$ is the BS wave function.

The solution of Eq. (5) is renormalized according to $S(p)^{-1} = i\not{p} + m(\mu)$ at a sufficiently large spacelike μ^2, with $m(\mu)$ the renormalized quark mass at the scale μ. In Eq. (5), S, Γ_μ^i, and $m(\mu)$ depend on the quark flavor, although we have not indicated this explicitly. The renormalization constants Z_2 and Z_4 depend on the renormalization point and the regularization mass scale, but not on flavor: in our analysis we employ a flavor-independent renormalization scheme.

The meson BSAs $\Gamma^{a\bar{b}}(q,q';P)$ are normalized according to the canonical normalization condition

$$\begin{aligned}2\,P_\mu = N_c \frac{\partial}{\partial P_\mu}\int^\Lambda \frac{d^4q}{(2\pi)^4}\Bigg\{ & \mathrm{Tr}[\bar{\Gamma}^{a\bar{b}}(\tilde{q}',\tilde{q};-Q) \\ & \times S^a(q+\eta P)\,\Gamma^{a\bar{b}}(\tilde{q},\tilde{q}';Q)\,S^b(q+(\eta-1)P)] \\ & + \int^\Lambda \frac{d^4k}{(2\pi)^4}\mathrm{Tr}[\bar{\chi}^{a\bar{b}}(\tilde{k}',\tilde{k};-Q) \\ & \times K(\tilde{k},\tilde{q};P)\,\chi^{a\bar{b}}(\tilde{q},\tilde{q}';Q)]\Bigg\},\end{aligned} \tag{7}$$

at the mass shell $P^2=Q^2=-m^2$, with $\tilde{q}=q+\eta Q$, $\tilde{q}'=q+(\eta-1)Q$, and similarly for $\tilde{k}$ and $\tilde{k}'$. We use the conventions where $f_\pi = 131$ MeV, and η describes the momentum partitioning between the quark and antiquark. Note that physical observables should be independent of this parameter.

For pseudoscalar bound states the BSA is commonly decomposed into [2]

$$\begin{aligned}\Gamma(k+\eta P,k+(\eta-1)P;P) = \gamma_5[& iE(k^2,k\cdot P;\eta) \\ & + \not{P}\,F(k^2,k\cdot P;\eta) \\ & + \not{k}\,G(k^2,k\cdot P;\eta) \\ & + \sigma_{\mu\nu}k_\mu P_\nu H(k^2,k\cdot P;\eta)],\end{aligned} \tag{8}$$

where the invariant amplitudes E, F, G, and H are Lorentz scalar functions of k^2 and $k\cdot P = kP\cos\theta$. The dependence of the amplitudes upon $k\cdot P$ can be conveniently represented by the following expansion based on Chebyshev polynomials:

$$f(k^2,k\cdot P;P^2) = \sum_{i=0}^{\infty} U_i(\cos\theta)(kP)^i f_i(k^2;P^2). \tag{9}$$

For charge-parity eigenstates such as the pion, each amplitude E, F, G, and H will have a well-defined parity in the variable $k\cdot P$ if one chooses $\eta=\frac{1}{2}$. In this case, these amplitudes are either entirely even (E, F, and H) or odd (G) in

[1] We use Euclidean metric $\{\gamma_\mu,\gamma_\nu\}=2\delta_{\mu\nu}$, $\gamma_\mu^\dagger=\gamma_\mu$, and $a\cdot b = \sum_{i=1}^4 a_i b_i$.

$k\cdot P$, and only the even or odd Chebyshev moments f_i are needed for a complete description.

B. The quark-photon vertex

The quark-photon vertex is the solution of the renormalized inhomogeneous BSE with the same kernel K as the homogeneous BSE for meson bound states. That is

$$\Gamma^a_\mu(p_+,p_-;Q)=Z_2\ \gamma_\mu+\int^\Lambda \frac{d^4q}{(2\pi)^4}\ K(p,q;Q) \times S^a(q_+)\ \Gamma^a_\mu(q_+,q_-;Q)\ S^a(q_-), \tag{10}$$

with $p_\pm=p\pm\frac{1}{2}Q$ and $q_\pm=q\pm\frac{1}{2}Q$. Because of gauge invariance, it satisfies the Ward-Takahashi identity (WTI)

$$i\,Q_\mu\,\Gamma^a_\mu(p_+,p_-;Q)=S_a^{-1}(p_+)-S_a^{-1}(p_-). \tag{11}$$

Solutions of the homogeneous version of Eq. (10) at discrete timelike momenta Q^2 define vector meson bound states with masses $m_V^2=-Q^2$. It follows that Γ^a_μ has poles at those locations and, in the vicinity of the bound states, behaves similar to [7]

$$\Gamma^a_\mu(p_+,p_-;Q)\to\frac{\Gamma^{a\bar{a}\,V}_\mu(p_+,p_-;Q)f_V m_V}{Q^2+m_V^2}, \tag{12}$$

where $\Gamma^{a\bar{a}\,V}_\mu$ is the $a\bar{a}$ vector meson BSA, and f_V is the electroweak decay constant.

For the photon coupled to u and d quarks, this results in a ρ-meson pole at $Q^2=-0.6\,\mathrm{GeV}^2$. For the photon coupled to s quarks, the first pole is located around $Q^2=-1.0\,\mathrm{GeV}^2$ at the ϕ mass. At the level of the ladder approximation, which is commonly used in practical calculations, there is no width generated for the vector mesons, and the vertex poles are located at real timelike values of Q^2. For example, one would have to supplement the ladder BSE kernel with the $\pi\pi$ production mechanism to produce a ρ-meson width for the corresponding vertex pole beyond the threshold for pion production, $Q^2<-4\,m_\pi^2$ in the timelike region.

The full vertex Γ^a_μ can be decomposed into four longitudinal components and eight transverse components. The longitudinal components do not contribute to the form factors. In Ref. [6] it was shown that only five of the eight transverse components are important for the pion form factor in the range $-0.3<Q^2<1.0\,\mathrm{GeV}^2$, with the remaining three components contributing less than 1%. We expect that this will also be the case for the kaon form factor, and use the Dirac amplitudes T_1 to T_5 of Ref. [6] only.

C. Charge conservation

At $Q=0$ the quark-photon vertex is completely specified by the differential Ward identity

$$i\,\Gamma^b_\mu(p,p;0)=\frac{\partial}{\partial p_\mu}S_b^{-1}(p). \tag{13}$$

If this is inserted in Eq. (4), one finds after a change of integration variables $k\to k-\frac{1}{2}P$

$$\Lambda^{a\bar{b}b}_\nu(P,0)=2P_\mu F_{a\bar{b}b}(0)=N_c\int^\Lambda\frac{d^4q}{(2\pi)^4}\mathrm{Tr}\left[\bar{\Gamma}^{a\bar{b}}(q',q;P)\,S^a(q)\,\Gamma^{a\bar{b}}(q,q';P)\,\frac{\partial S^b(q-P)}{\partial P_\mu}\right], \tag{14}$$

with $q'=q-P$. Comparing this expression to Eq. (7) with $\eta=0$, we recognize that the physical result $F(Q^2=0)=1$ follows directly from the canonical normalization condition for $\Gamma^{a\bar{b}}$ if the BSE kernel K is independent of the meson momentum P. For the ladder truncation of the kernel, which we consider in our calculation in the next section, this is the case.

With an arbitrary value for the momentum partitioning parameter η, the relation between the normalization condition for Γ^{ab} and electromagnetic current conservation is not so straightforward. A shift in the value of η in loop diagrams (without external quark lines) is equivalent to a shift in integration variables. For processes that are not anomalous, loop integrals are independent of a shift in integration variables provided that all approximated quantities in the integrand respect Poincaré invariance. In this respect, particular attention must be paid to the representation and approximation used for the BSAs. The general BSE vertex solution $\Gamma(q,q';P)$, considered as a function of the incoming and outgoing quark momenta, does not depend on η. It is only in commonly used decompositions in terms of Lorentz invariant amplitudes, such as Eq. (8), that the value of η becomes relevant. The amplitudes E, F, G, and H are scalar functions of k^2 and $k\cdot P$ which *do* depend on η, i.e., on the choice of a relative momentum. Under a change of η, some of the different Dirac covariants and associated amplitudes (such as F and G) will mix. So will the various Chebyshev moments f_i in Eq. (9). However, the net result from use of a complete representation of both the Dirac matrix structure and the $k\cdot P$ variable is independent of η and the momentum routing in loop integrals. Previously it has been shown that under these conditions the decay constants are indeed independent of η [2].

With dressed propagators, the use of a bare quark-photon vertex in Eq. (4) clearly violates charge conservation and leads to $F_\pi(0)\neq 1$. Use of the Ball-Chiu ansatz [11] for the dressed quark-photon vertex, a common element in past DSE

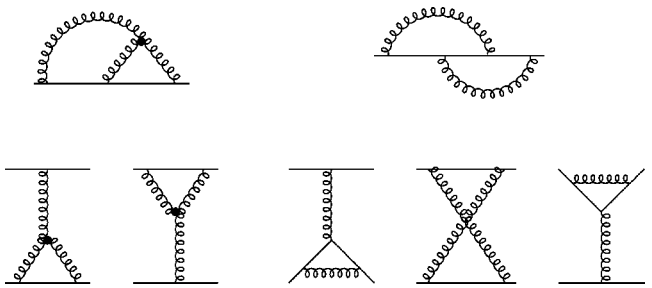

FIG. 1. The two leading-order vertex corrections to the rainbow DSE (top) and the corresponding five diagrams to be added to the ladder BSE kernel (bottom) for consistency with the relevant WTIs. The quark and gluon lines indicate dressed propagators in this and the subsequent figures.

studies of electromagnetic interactions [12–17], conserves the electromagnetic current and ensures $F(Q^2=0)=1$. However, the behavior of the form factor away from $Q^2=0$ is not constrained by current conservation, and in the present model, use of the Ball-Chiu ansatz leads to a value for r_π^2 which is about 50% too small [6]. With the quark-photon vertex produced by solution of the ladder BSE, and with quark propagators from the rainbow DSE, all constraints from current conservation are satisfied and the calculated value of r_π^2 is within 5% of the experimental value [6].

D. Beyond rainbow-ladder truncation

If one goes beyond the rainbow-ladder truncation for the DSEs for the propagators, BSAs and quark-photon vertex, one has to go beyond impulse approximation for the form factors to ensure current conservation. For example, one could include corrections to the rainbow-ladder DSE and BSE kernels that are higher-order in α_s, as depicted in Fig. 1. Following the general procedure developed in Ref. [18], one can show that both the WTI, Eq. (11), and the differential Ward identity, Eq. (13), are preserved in the truncation indicated in Fig. 1. Also preserved is the axial-vector WTI, which is important for the Goldstone nature of the pions.

The resulting BSE kernel $K(q,p;P)$ now becomes dependent on the meson momentum P, which means that the second term of the normalization condition, Eq. (7), is nonzero. To be specific, with the choice $\eta=0$, this introduces the four extra terms in the normalization condition depicted in Fig. 2.

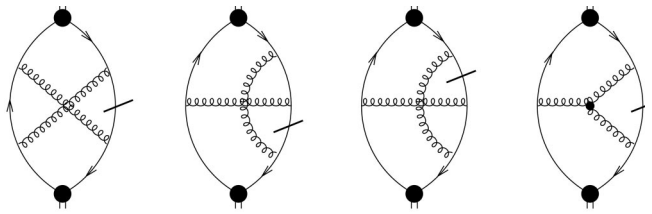

FIG. 2. The four diagrams arising from the P dependence of the kernel in the normalization condition, Eq. (7), if one includes the diagrams of Fig. 1 into the DSE dynamics, and chooses all of the meson momentum P to flow through one quark only. The derivatives with respect to P are marked by slashes.

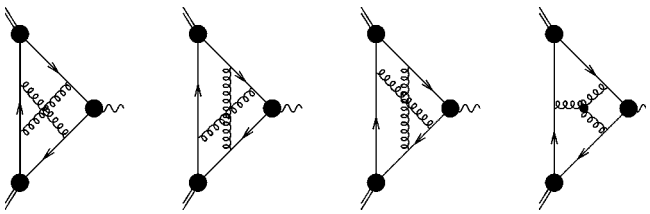

FIG. 3. The four corrections to the impulse approximation, Eq. (4), necessary to maintain current conservation if one includes the diagrams of Fig. 1 into the DSE dynamics.

These four additional diagrams are generated from the BSE kernel in the bottom part of Fig. 1 by taking the derivative with respect to the meson momentum P, where P flows through one quark propagator only.

Since a derivative with respect to P is equivalent to the insertion of a zero-momentum photon according to the differential WTI, Eq. (11), it is obvious which diagrams have to be added to the impulse approximation for the vertex $\Lambda^{a\bar{b}b}$ to maintain current conservation, see Fig. 3. In the limit $Q\to 0$ these four additional diagrams become identical to the four additional diagrams in Fig. 2, provided that the vertex satisfies the differential WTI. Of course, there are similar contributions to $\Lambda^{a\bar{b}a}$, which can be identified with terms in the normalization condition with $\eta=1$.

A related topic is the correction to the impulse approximation from pion and kaon loops. Simple addition of such loops without supplementing the ladder-rainbow truncation for the DSEs, will generally violate current conservation. A consistent treatment of the kernels for both the DSE and BSE equations and the approximation for the photon-hadron coupling is necessary for current conservation. At present it is not clear how to incorporate meson loops self-consistently in such an approach, but we expect corrections coming from such loops to be small in the spacelike region. In Ref. [19] it was demonstrated that the dressed quark core can generate most of the pion charge radius, and that pion loops contribute less than 15% to r_π^2. For larger values of Q^2 the effect from meson loops reduces even further, and for $Q^2>1\ \mathrm{GeV}^2$ we expect the contribution of such loops to be negligible.

III. MODEL CALCULATIONS

We employ the model that has been developed recently for an efficient description of the masses and decay constants of the light pseudoscalar and vector mesons [2,7]. This consists of the rainbow truncation of the DSE for the quark propagator and the ladder truncation of the BSE for the pion and kaon amplitudes. The required effective $\overline{qq}$ interaction is constrained by perturbative QCD in the ultraviolet and has a phenomenological infrared behavior. In particular, the ladder truncation of the BSE, Eq. (6), is

$$K(p,q;P)\to -\mathcal{G}(k^2)\,D_{\mu\nu}^{\mathrm{free}}(k)\,\frac{\lambda^i}{2}\gamma_\mu\otimes\frac{\lambda^i}{2}\gamma_\nu, \qquad (15)$$

where $D_{\mu\nu}^{\mathrm{free}}(k=p-q)$ is the free gluon propagator in Landau gauge. The consistent rainbow truncation of the quark DSE,

TABLE I. Overview of the results of the model for the meson masses and decay constant, adapted from Refs. [2,7]. The experimental value for the condensate is taken from Ref. [21].

	experiment [22] (estimates)	calculated († fitted)
$m^{u=d}_{\mu=1\ \mathrm{GeV}}$	5–10 MeV	5.5 MeV
$m^{s}_{\mu=1\ \mathrm{GeV}}$	100–300 MeV	125 MeV
$-\langle\bar{q}q\rangle^0_\mu$	$(0.236\ \mathrm{GeV})^3$	$(0.241^\dagger)^3$
m_π	0.1385 GeV	$0.138^\dagger$
f_π	0.131 GeV	$0.131^\dagger$
m_K	0.496 GeV	$0.497^\dagger$
f_K	0.160 GeV	0.155
m_ρ	0.770 GeV	0.742
f_ρ	0.216 GeV	0.207
$m_{K^\star}$	0.892 GeV	0.936
$f_{K^\star}$	0.225 GeV	0.241
m_ϕ	1.020 GeV	1.072
f_ϕ	0.236 GeV	0.259

Eq. (5), is given by $\Gamma^i_\nu(q,p)\rightarrow\ \gamma_\nu\lambda^i/2$ together with $g^2D_{\mu\nu}(k)\rightarrow\ \mathcal{G}(k^2)D^{\mathrm{free}}_{\mu\nu}(k)$. These two truncations are consistent in the sense that the combination produces vector and axial-vector vertices satisfying the respective WTIs. In the axial case, this ensures that in the chiral limit the ground state pseudoscalar mesons are the massless Goldstone bosons associated with chiral symmetry breaking [2,10]. In the vector case, this ensures electromagnetic current conservation.

The model is completely specified once a form is chosen for the ''effective coupling'' $\mathcal{G}(k^2)$. The ultraviolet behavior is chosen to be that of the QCD running coupling $\alpha(k^2)$; the ladder-rainbow truncation then generates the correct perturbative QCD structure of the DSE-BSE system of equations. The phenomenological infrared form of $\mathcal{G}(k^2)$ is chosen so that the DSE kernel contains sufficient infrared enhancement to produce an empirically acceptable amount of dynamical chiral symmetry breaking as represented by the chiral condensate [20].

We employ the ansatz found to be successful in earlier work [2,7]

$$\frac{\mathcal{G}(k^2)}{k^2}=\frac{4\pi^2 D\,k^2}{\omega^6}e^{-k^2/\omega^2}+\frac{4\pi^2\,\gamma_m\ \mathcal{F}(k^2)}{\frac{1}{2}\ln[\,\tau+(1+k^2/\Lambda^2_{\mathrm{QCD}})^2]}, \tag{16}$$

with $\gamma_m=12/(33-2N_f)$ and $\mathcal{F}(s)=[1-\exp(-s/4m_t^2)]/s$. This ansatz preserves the one-loop renormalization group behavior of QCD, and the first term implements the strong infrared enhancement in the region $0<k^2<1$ GeV^2 required for sufficient dynamical chiral symmetry breaking. We use $m_t=0.5$ GeV, $\tau=e^2-1$, $N_f=4$, $\Lambda_{\mathrm{QCD}}=0.234$ GeV, and a renormalization scale $\mu=19$ GeV which is well into the domain where one-loop perturbative behavior is appropriate [2,7]. The remaining parameters, $\omega=0.4$ GeV and $D=0.93$ GeV^2 along with the quark masses, are fitted to give a good description of the chiral condensate, $m_{\pi/K}$ and f_π. The subsequent values for f_K and the masses and decay constants of the vector mesons $\rho,\phi,K^\star$ are in agreement with the experimental data [7], see Table I.

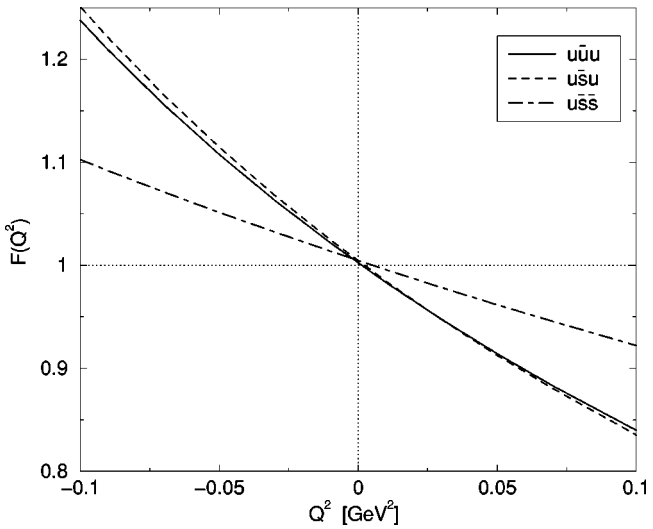

FIG. 4. The three independent form factors $F_{u\bar{u}u}$, $F_{\bar{u}su}$, and $F_{\bar{u}s\bar{s}}$.

A detailed analysis of the relationship between QCD and this Landau gauge, renormalization-group-improved, rainbow-ladder truncation of the DSEs can be found in the originating work [2] and in several recent reviews [3,23]. These reviews also provide provide a wider perspective that includes a compilation of results for both meson and baryon physics, an analysis how quark confinement is manifest in solutions of the DSEs, and a comparison with lattice QCD results [24] that confirm the qualitative behavior for the dressed quark propagator produced by DSE models of the present type. The question of the accuracy of the ladder-rainbow truncation has also received some attention; it was found to be particularly suitable for the flavor octet pseudoscalar mesons since the next-order contributions in a quark-gluon skeleton graph expansion, have a significant amount of cancellation between repulsive and attractive corrections [18].

A. Results for $u\bar{u}u$, $\bar{u}su$, and $\bar{u}s\bar{s}$ form factors

The pion and kaon form factors are given by

$$F_\pi(Q^2)=\tfrac{2}{3}F_{u\bar{d}u}(Q^2)+\tfrac{1}{3}F_{u\bar{d}\bar{d}}(Q^2), \tag{17}$$

$$F_{K^+}(Q^2)=\tfrac{2}{3}F_{\bar{u}su}(Q^2)+\tfrac{1}{3}F_{\bar{u}s\bar{s}}(Q^2), \tag{18}$$

$$F_{K^0}(Q^2)=-\tfrac{1}{3}F_{d\bar{s}d}(Q^2)+\tfrac{1}{3}F_{d\bar{s}\bar{s}}(Q^2), \tag{19}$$

where the quark and antiquark charges are evident. We work in the SU(2) isospin limit, where the strong interaction does not discriminate between u and d quarks, so for the pion we simply have $F_\pi(Q^2)=F_{u\bar{u}u}(Q^2)$. Thus there are only three independent form factors, $F_{u\bar{u}u}(Q^2)$, $F_{\bar{u}su}(Q^2)$, and $F_{\bar{u}s\bar{s}}(Q^2)$, which are shown in Fig. 4. Our estimate of the numerical error in these calculations is less than 1% for $F_{u\bar{u}u}(Q^2)$, and 2% for the other two form factors.

TABLE II. Our results for the charge radii, compared with the experimental values given in Refs. [25–27].

charge radii	experiment		calculated	
r_π^2	0.44 ± 0.01	fm^2	0.45	fm^2
$r_{K^+}^2$	0.34 ± 0.05	fm^2	0.38	fm^2
$r_{K^0}^2$	-0.054 ± 0.026	fm^2	-0.086	fm^2

For the pion we use only the leading terms of the $k \cdot P$ expansion of the BSAs and the quark-photon vertex given in Eq. (9). Higher order terms do not change the results more than 1% in this momentum regime, although they are needed at larger values of Q^2. For the kaon we have to use more terms in the expansion, even at $Q^2=0$, to obtain independence from the parameter η, and to ensure current conservation. With terms up to order $(k \cdot P)^1$ only, there is a spread in our results of more than 10% at $Q^2=0$ (from 0.94 to 1.06) if we change η between 0 and 1. With the next two terms included, that spread is reduced to less than 3%. This illustrates that the impulse approximation is independent of the unphysical parameter η, provided that all relevant Dirac structures and the complete dependence on $k \cdot P$ are properly taken into account.

The results for $F_{u\bar{u}u}$ and $F_{u\bar{s}u}$ are remarkably close to each other, indicating that the flavor of the spectator quark matters very little. Within our numerical errors, they are almost indistinguishable on the Q^2 domain shown. There is a slight difference in the slope of these form factors: $r^2_{u\bar{u}u} = 0.45$ fm^2 versus $r^2_{u\bar{s}u} = 0.47$ fm^2. These results are in good agreement with the pion charge radius $r_\pi^2 = 0.46$ fm^2, obtained in Ref. [6] using all eight Dirac amplitudes of the quark-photon vertex.

The result for $F_{u\bar{s}\,\bar{s}}$ is quite different in that it has a significantly smaller slope characterized by a radius parameter $r^2_{u\bar{s}\,\bar{s}} = 0.21$ fm^2. This is due to the larger mass of the strange quark, and as a consequence the neutral kaon charge radius $r_{K^0}^2$ will be negative. A similar effect was observed for the neutron form factor, where the heavier mass of the $0^+(ud)$ diquark compared to the d quark mass leads to a negative charge radius [17]. Our result is also consistent with the qualitative aspects of the vector meson dominance (VMD) picture: the lowest-mass bound state pole in the $ss\gamma$ vertex is the ϕ, at $Q^2=-1.0$ GeV^2, which is significantly further from the photon point than is the ρ pole in the $uu\gamma$ vertex at $Q^2=-0.6$ GeV^2. This observation, as well as the difference between $r^2_{u\bar{s}\,\bar{s}}$ and $r^2_{u\bar{s}u}$, is consistent with the larger mass of the strange quark.

B. Results for the meson form factors

The results in this model for the pion form factor at low Q^2, in particular the pion charge radius, were presented previously [6]. The obtained charge radii for the kaon are presented in Table II, and are in reasonable agreement with the experimental data, without any readjustment of the model. In Fig. 5 we show our result for the charged kaon form factor which is in good agreement with the available data.

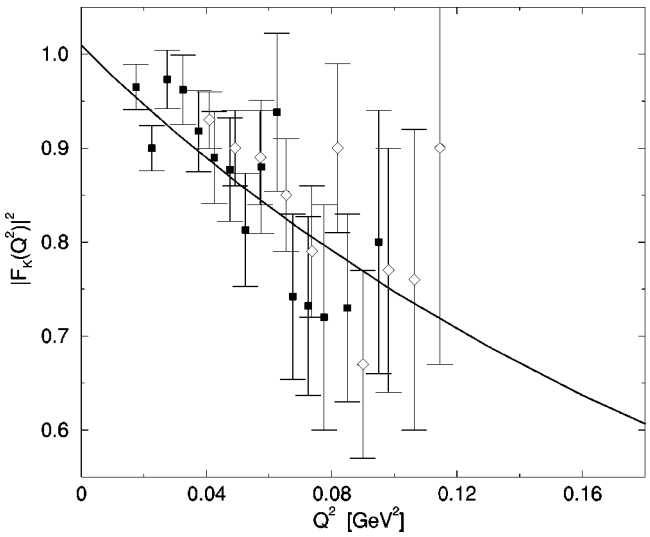

FIG. 5. The calculated K^+ form factor compared to the data from Refs. [28] (open diamonds) and [26] (solid squares). Within numerical errors $|F_{K^+}(0)|^2=1$.

Finally, in Fig. 6 we present $Q^2F(Q^2)$ for π and $K^{0,\pm}$ for a larger Q^2 range to anticipate data that may be forthcoming from experiments at JLab [4,5] and possibly other facilities in the future. In this momentum range, even for $F_\pi(Q^2)$ the dependence on $k \cdot P$ becomes important, and terms up to $(k \cdot P)^3$ in Eq. (9) are required to produce a converged result

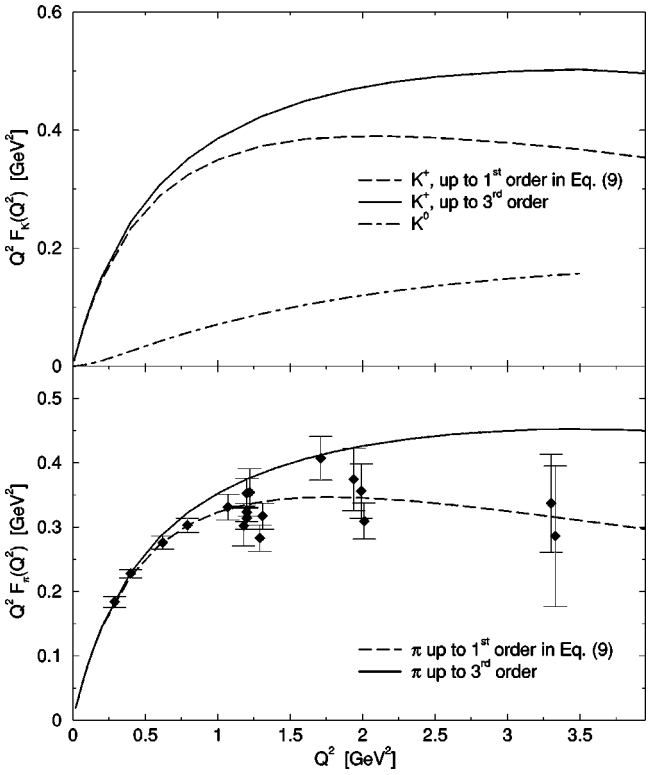

FIG. 6. Q^2 times the kaon form factors (top) and pion form factor (bottom). The pion data are from Ref. [29].

at $Q^2=1\sim3\,\mathrm{GeV}^2$. Higher-order terms do not change the results by more than 1% in this momentum range. Our estimate is that the net numerical accuracy for $F_{u\bar{u}u}$, $F_{u\bar{s}u}$, and $F_{us\bar{s}}$ is about 2–3 % at these values of Q^2. This translates to a similar level of accuracy for F_π and F_{K^+}, and to a somewhat larger relative error, about 5%, for F_{K^0}, which is the difference of $F_{us\bar{s}}$ and $F_{u\bar{s}u}$. At $Q^2>3\,\mathrm{GeV}^2$, higher-order Chebyshev moments may be necessary, but current numerical methods prevent their accurate determination at large Q^2.

Over the entire spacelike momentum range considered, $F_\pi(Q^2)<F_{K^+}(Q^2)$, and $Q^2F(Q^2)$ rises with Q^2 until $Q^2=3\,\mathrm{GeV}^2$ for all three form factors. In this momentum range our results for both the pion and the K^+ form factor can be fitted quite well by a simple monopole $m^2/(Q^2+m^2)$, with a mass $m^2=0.53\,\mathrm{GeV}^2$ for the pion and $m^2=0.61\,\mathrm{GeV}^2$ for the K^+. A VMD model, in which the two form factors $F_{u\bar{s}u}$ and $F_{us\bar{s}}$ in Eqs. (18) and (19) are represented by separate monopoles with the physical ρ and ϕ masses, respectively, does not reproduce our results for the kaon form factors very well. For example, at $Q^2=1\,\mathrm{GeV}^2$, VMD overshoots our F_{K^+} calculation by almost 10%, whereas the single monopole fit is within 2% of our result. This difference between VMD and our calculations grows with Q^2.

Above $Q^2\sim3.5\,\mathrm{GeV}^2$ our results indicate $Q^2F(Q^2)$ is starting to decrease and the monopole fits cease to be an adequate representation. In a more complete description that takes meson loop corrections into account self-consistently, it is quite conceivable that this turn-over begins at somewhat lower values of Q^2. This is likely because meson loops are expected to increase r_π^2 by up to 15% [19] while having rapidly decreasing influence with increasing spacelike momenta. Thus in the presence of consistent meson loop corrections, the impulse approximation would need to yield a smaller form factor than our present result if agreement with the low-Q^2 data is to be maintained. It is therefore possible that the present approach overestimates the form factors at intermediate momenta and this may explain the discrepancy with the data near $Q^2=3\,\mathrm{GeV}^2$. More accurate results from JLab, in combination with realistic model calculations that include self-consistent meson loop corrections, may be able to resolve this question.

At asymptotically large Q^2, factorized pQCD [30] predicts that the form factor behaves as $Q^2F(Q^2)\to c$, with $c=8\pi f_\pi^2\alpha_s(Q^2)$. Since our truncation and the ansatz, Eq. (16), is constructed so as to preserve asymptotic freedom, we are guaranteed to recover the leading power-law asymptotic behavior. An explicit verification of this behavior, and calculation of the constant c, is not readily available within our present framework since numerical accuracy at such large Q^2 is problematic. However, it is clear from our results that at $Q^2\sim4\,\mathrm{GeV}^2$ the form factor has not yet reached its asymptotic value, and it is unlikely that experiments can access the true asymptotic region in the near future. In simplified models such as that of Ref. [15] however, it is straightforward to demonstrate that the impulse approximation does indeed lead to the power-law behavior predicted by PQCD.

IV. SUMMARY

We calculate the pion and kaon electromagnetic form factors within the DSE approach. The method is completely Poincaré invariant, and the only approximation made is a self-consistent truncation of the set of DSEs, which respects the relevant vector and axial-vector WTIs. The employed quark propagators, the meson BSAs, and the quark-photon vertex are solutions of their DSEs in rainbow-ladder truncation with all parameters fixed previously by fitting the chiral condensate, $m_{\pi/K}$ and f_π. We include all relevant Dirac amplitudes for the BSAs and their full dependence upon $k\cdot P$. The electromagnetic current is explicitly conserved in this approach, and there is no fine-tuning needed to obtain $F_\pi(0)=1=F_{K^+}(0)$ and $F_{K^0}(0)=0$. We also demonstrate explicitly that our results are (within numerical accuracy) independent of the momentum partitioning of the BSAs. The obtained pion and kaon form factors are in good agreement with the available data over the entire Q^2 range considered, and the calculated charge radii are within the error bars of their experimental values.

These charge radii are somewhat larger than those obtained in a previous study [13] that was framed in terms of semiphenomenological representations for BSAs and confined quark propagators within the impulse approximation. The main difference with that work is that here we use numerical solutions of truncated DSEs for all the elements needed in Eq. (4), and that all our parameters were fixed previously. In comparison with theoretical calculations based on other methods, it is interesting to note that our results are very similar to those obtained in Ref. [31], in particular for the neutral kaon.

At intermediate values of Q^2 our calculations are qualitatively similar to those obtained in both Refs. [13,31]. Up to about $Q^2=3\,\mathrm{GeV}^2$, both F_π and F_{K^+} can be fitted quite well by a monopole form, with monopole masses of $m^2=0.53\,\mathrm{GeV}^2$ and $m^2=0.61\,\mathrm{GeV}^2$, respectively. At large Q^2 the DSE approach does reproduce the pQCD power-law behavior [30], but this behavior does not occur until well beyond [15] the Q^2 range considered in our present calculations and accessible at current accelerators.

ACKNOWLEDGMENTS

We acknowledge useful conversations and correspondence with C.D. Roberts, D. Jarecke, and S.R. Cotanch. This work was funded by the National Science Foundation under Grant No. PHY97-22429, and benefited from the resources of the National Energy Research Scientific Computing Center.

[1] See, e.g., H.J. Munczek and D.W. McKay, Phys. Rev. D **39**, 888 (1989); D. Atkinson, H.J. de Groot, and P.W. Johnson, *ibid.* **43**, 218 (1991); H.J. Munczek and P. Jain, *ibid.* **46**, 438 (1992); M.R. Frank and C.D. Roberts, Phys. Rev. C **53**, 390 (1996).
[2] P. Maris and C.D. Roberts, Phys. Rev. C **56**, 3369 (1997).
[3] C.D. Roberts and S.M. Schmidt, nucl-th/0005064; R. Alkofer and L. von Smekal, hep-ph/0007355.
[4] JLab experiment E93-018, spokesperson O.K. Baker.
[5] JLab experiment E93-021 and extension, spokespersons H. Blok, G. Huber, and D. Mack.
[6] P. Maris and P.C. Tandy, Phys. Rev. C **61**, 045202 (2000).
[7] P. Maris and P.C. Tandy, Phys. Rev. C **60**, 055214 (1999).
[8] C.J. Burden, C.D. Roberts, and A.G. Williams, Phys. Lett. B **285**, 347 (1992); G. Krein, C.D. Roberts, and A.G. Williams, Int. J. Mod. Phys. A **7**, 5607 (1992); P. Maris, Phys. Rev. D **52**, 6087 (1995).
[9] See, e.g., K. Higashijima, Phys. Rev. D **29**, 1228 (1984); V.A. Miransky, Phys. Lett. **165B**, 401 (1985); D. Atkinson and P.W. Johnson, Phys. Rev. D **37**, 2290 (1988); **37**, 2296 (1988); C.D. Roberts and B.H. McKellar, *ibid.* **41**, 672 (1990).
[10] P. Maris, C.D. Roberts, and P.C. Tandy, Phys. Lett. B **420**, 267 (1998).
[11] J.S. Ball and T.W. Chiu, Phys. Rev. D **22**, 2542 (1980).
[12] C.D. Roberts, Nucl. Phys. **A605**, 475 (1996).
[13] C.J. Burden, C.D. Roberts, and M.J. Thomson, Phys. Lett. B **371**, 163 (1996).
[14] P.C. Tandy, Prog. Part. Nucl. Phys. **39**, 117 (1997), and references therein.
[15] P. Maris and C.D. Roberts, Phys. Rev. C **58**, 3659 (1998).
[16] F.T. Hawes and M.A. Pichowsky, Phys. Rev. C **59**, 1743 (1999).
[17] J.C.R. Bloch, C.D. Roberts, S.M. Schmidt, A. Bender, and M.R. Frank, Phys. Rev. C **60**, 062201 (1999).
[18] A. Bender, C.D. Roberts, and L. von Smekal, Phys. Lett. B **380**, 7 (1996).
[19] R. Alkofer, A. Bender, and C.D. Roberts, Int. J. Mod. Phys. A **10**, 3319 (1995).
[20] F.T. Hawes, P. Maris, and C.D. Roberts, Phys. Lett. B **440**, 353 (1998).
[21] D.B. Leinweber, Ann. Phys. (N.Y.) **254**, 328 (1997).
[22] Particle Data Group, C. Caso *et al.*, Eur. Phys. J. C **3**, 1 (1998).
[23] C.D. Roberts, nucl-th/0007054.
[24] J.I. Skullerud and A.G. Williams, hep-lat/0007028.
[25] S.R. Amendolia *et al.*, Nucl. Phys. **B277**, 168 (1986).
[26] S.R. Amendolia *et al.*, Phys. Lett. B **178**, 453 (1986).
[27] W.R. Molzon *et al.*, Phys. Rev. Lett. **41**, 1213 (1978).
[28] E.B. Dally *et al.*, Phys. Rev. Lett. **45**, 232 (1980).
[29] C.J. Bebek *et al.*, Phys. Rev. D **17**, 1693 (1978).
[30] G.R. Farrar and D.R. Jackson, Phys. Rev. Lett. **43**, 246 (1979); G.P. Lepage and S.J. Brodsky, Phys. Rev. D **22**, 2157 (1980).
[31] H-M. Choi and C-R. Ji, Phys. Rev. D **59**, 074015 (1999).